PROCEEDINGS, 44th Workshop on Geothermal Reservoir Engineering
Stanford University, Stanford, California, February 11-13, 2019
SGP-TR-214

Geophysical Characterization of the heat source in the Northwest Geysers, California

Jared R. Peacock[1], Margaret T. Mangan[1], Mark Walters[2], Craig Hartline[2], Jonathan Glen[1], Tait Earney[1], William Schermerhorn[1]

[1]U.S. Geological Survey, 345 Middlefield Rd., Menlo Park, CA, [2]Calpine Corporation, 10350 Socrates Mine Road, Middletown, CA 95461

jpeacock@usgs.gov, mmangan@usgs.gov, craig.hartline@calpine.com, mark.walters@calpine.com, jglen@usgs.gov, tearney@usgs.gov, wschermerhorn@usgs.gov

Keywords: The Geysers, magnetotellurics, resistivity, gravity, three-dimensional modeling, EGS, HDR

ABSTRACT

The Geysers, in northern California, is the largest energy producing geothermal field in the world. Looking to expand capacity, the operator Calpine Corporation developed an anomalously hot (~400 °C at 2.5 km depth) part of the field in the northwest Geysers, including testing of an enhanced geothermal systems (EGS). Though the area is anomalously hot, geophysical methods have failed to adequately image any inferred magmatic heat source. Gravity measurements were collected and jointly modeled with existing magnetic data along a two-dimensional profile aligned with an existing geologic cross-section. The key feature of the potential field model is a low-density, low-susceptibility body below the EGS at 5 km depth. Magnetotelluric (MT) measurements were collected around the northwest Geysers and modeled in three-dimensions to characterize subsurface resistivity structure. The resistivity model images an extension of a Quaternary granitic pluton locally known as "the felsite" under the EGS project and a possible zone of partial melt (<10%) below 7 km in the northwestern part of the field.

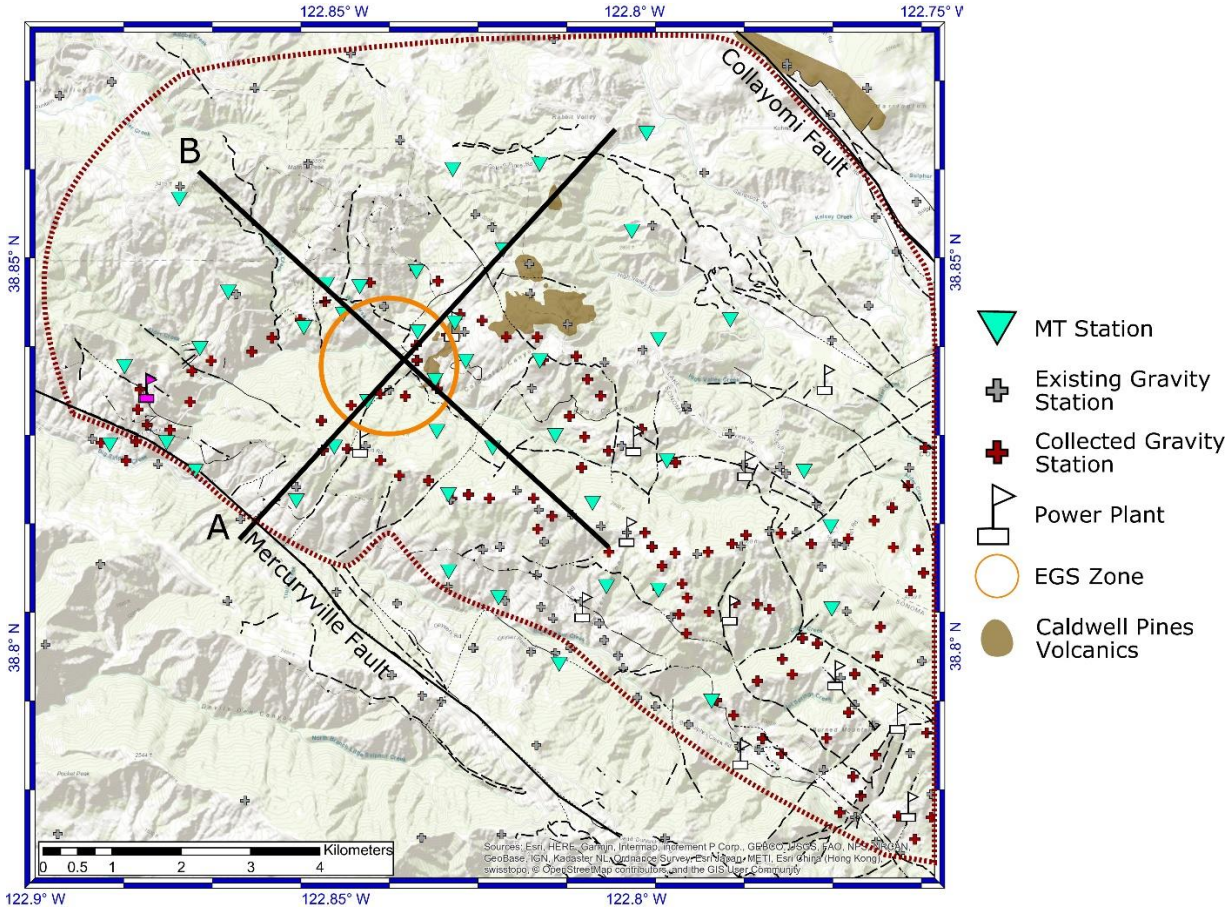

Figure 1: Map of MT and gravity stations. Profile lines A and B are thick black lines. The general outline of The Geysers geothermal field is dotted red line. Faults are thin black lines. The Aidlin power plant is represented as magenta power plant symbol.

1. INTRODUCTION

In northern California resides the world's largest energy producing geothermal field, The Geysers. Heat is provided by a series of shallow silicic intrusions (1 Ma – 10 ka) locally known as the 'felsite' (Schriener and Suemnicht, 1981). Energy production at The Geysers exploits a fracture-dominated natural steam field (235 °C) hosted mainly in a shallow (<2km) metagraywacke reservoir (McLaughlin, 1978, 1981; Thompson and Cunderson, 1992). Since the late 1990's, treated waste water has been injected to help sustain energy production. The hottest region of The Geysers is in the northwestern geothermal field where temperatures reach 400 °C below 2.5 km (Figure 1). This hot dry rock reservoir (HDR) needs to be stimulated for energy production (Walters et al, 1992; Stimac et al., 2001).

Since 1976, an inadvertent enhanced geothermal system (EGS) has been developed in the northern part of The Geysers that has helped sustain production (Stark, 2003). To test this concept in detail, in 2011 and 5 km north of the inadvertently created EGS, Prati State 31 (PS-31) and Prati State 32 (PS-32) wells were reopened and deepened for usage as a production-injection pair to stimulate the HDR in the northwest Geysers (Garcia et al., 2012). The Northwest Geysers EGS has been stimulated, monitored (Boyle and Zoback, 2013; Vasco et al., 2013; Jeanne et al., 2015; Tezel et al., 2016), and modeled (Jeanne et al., 2014; Rutqvist et al., 2015; Rutqvist et al., 2016) since late 2011. The developed EGS is roughly between 2-4 km depth, is elongated in the N30E direction, and is producing steam that is 50-75% derived from injected fluids (Jeanne et al., 2014; Jeanne et al., 2015, Rutqvist et al., 2016; Garcia et al., 2016). The hope is that with further stimulation fluids will penetrate deeper towards the felsite and encounter hotter temperatures associated with recent granitic intrusions (Williams et al., 1993) for thermal mining (Rutqvist et al., 2016).

Heat flow models suggest small recent intrusions under the HDR (Williams et al, 1993; Stimac et al., 2001). Petrology of core from wells in the HDR include high-temperature veins of albite, biotite, clinopyroxene, pyrrhotite, quartz and tourmaline, and local sodium metasomatism suggestive of connate water or magmatic hydrothermal fluids (Lutz et al., 2012). However, to date the heat source for the HDR has not been imaged with geophysical methods. Seismicity tends to be confined to the top 5 km constraining seismic tomography models to similar depths (Julian et al., 1996; Gritto et al., 2013; Tezel et al., 2016; Lin & Wu, 2018). Models of potential field, electrical, and electromagnetic data have been focused mainly on regional structures and are too coarse to resolve small scale features like the intrusions under the HDR (Stanley et al., 1973; Denlinger and Kovach, 1981; Stanley and Blakely, 1995; Stanley et al., 1998). The goal of this study is to use newly collected magnetotelluric (MT) and gravity data to image the heat source of the HDR.

2. MT DATA

In the summer of 2017, 41 MT stations were collected around the northwest Geysers (Figure 1). MT data were recorded with ZEN 32-bit data loggers developed by Zonge International for an average of 20 hours with a repeating schedule of 7 hours and 50 minutes at 256 samples/second and 10 minutes at 4096 samples/second. ANT-4 induction coils from Geotell were used as magnetic sensors and Borin Ag-AgCl Fat Cat reference electrodes placed in saturated bags of bentonite clay were used as electric sensors. Induction coils and dipoles (50m, depending on topography and infrastructure), were set up in a T-configuration aligned with geomagnetic north. Most locations were old or operating well pads, therefore all MT stations only include the horizontal magnetic components and no vertical magnetic data was collected.

Data were processed with BIRRP (Chave and Thompson, 2004), where synchronous stations were used as remote references. For being in an electrically noisy area the MT response curves were relatively smooth, except at high frequencies consistent with electrical power transmission. Geoelectrical strike angles are random for periods smaller than 1 second and on average N45E for periods longer than 1 second, perpendicular to the Mercuryville and Collayomi Fault Zones. Phase tensor skew values range between ±6 degrees, with high skew values for periods greater than 1 second, suggesting the need for 3D modeling.

2.1 Modeling

MT data were modeled in 3D using the inversion code ModEM (Kelbert et al., 2014). The input data were interpolated onto the same 23 periods ranging from 0.02 – 1024 sec, where obvious outliers were removed using MTpy (Krieger & Peacock, 2014). The model grid included topography and the ocean. Cell size within the station area was 200 m and exponentially increased outside the station area and vertically downwards with a first layer of 5 m for a total model of 70 x 81 x 70 cells (350 x 350 x 250 km). The inversion was run in 2 steps to get a smooth model that fits the data. The first step was to invert the full impedance tensor with an error floor of 0.07 sqrt(Z_{xy} * Z_{yx}), a covariance of 0.4 in all directions applied once, a starting lambda of 10000, and a starting half-space of 100 Ohm-m. This converged after 83 iterations to a normalized RMS of 1.2. The second step was to use the converged model as a prior model, reduce the error floor to 0.03 sqrt(Z_{xy} * Z_{yx}), the covariance to 0.2 in all directions applied twice, and the starting lambda value to 100. This inversion converged after 57 iterations to a normalized RMS of 1.9. Many interesting features are observed in the 3D electrical resistivity model, however only 3 features will be discussed here. The main feature (R1) is a resistive body (>45 Ohm-m) that coincides with both the main steam field and the felsite. R2 is a northeast extension of R1 under the EGS (Figure 3). C1 is a conductive anomaly (<30 Ohm-m) that is under the EGS but has a possible extension towards the surface (Figure 4).

2. GRAVITY DATA

As part of the present study, 126 new gravity stations were collected in the Geysers Geothermal Area in September 2018, with a spacing of approximately 300 meters between sites (Figure 1). These data were combined with a much larger regional dataset containing many thousands of stations to provide regional coverage. Scintrex CG5 gravity meters were used to measure the observed gravity values along roadways and well pads. A base station in Clear Lake was used to account for instrument drift. Data were reduced to the isostatic gravity anomaly using the methods outlined in Blakely (1995), Godson & Plouff (1988), and Simpson et al., (1985).

3.1 Modeling

Gravity and aeromagnetic data (U.S. Geological Survey, 1996) were jointly modeled in 2D using Geosoft® GMSYS profile modeling software (Figure 2). The starting model was developed from the geologic cross section from Garcia et al. (2012) and iteratively changed to fit the data. Density, magnetic susceptibility, and magnetic remanence values were used from existing measurements (Blakely & Stanley, 1993; Stanley & Blakely, 1995; Lutz et al., 2012) and where unknown estimated from a database of similar lithologies. The upper 2 kilometers agree with most of the potential field data however, the long-wavelength aeromagnetic and gravity lows in the middle of the profile are sensitive to the deeper structures. A lower density (2.65 g/m^3) body below 5 km depth is needed to fit the data (the salmon body labeled "granite (Recent)"). This is interpreted as the Recent (<10 ka) intrusion heating the HDR. Note that the model shown in Figure 2 is very preliminary, however the key aspect of the model is that a low-density, low-susceptibility body (granite) is needed below 5 km depth to fit the data. The geometry of this granite is not well constrained and requires further modeling.

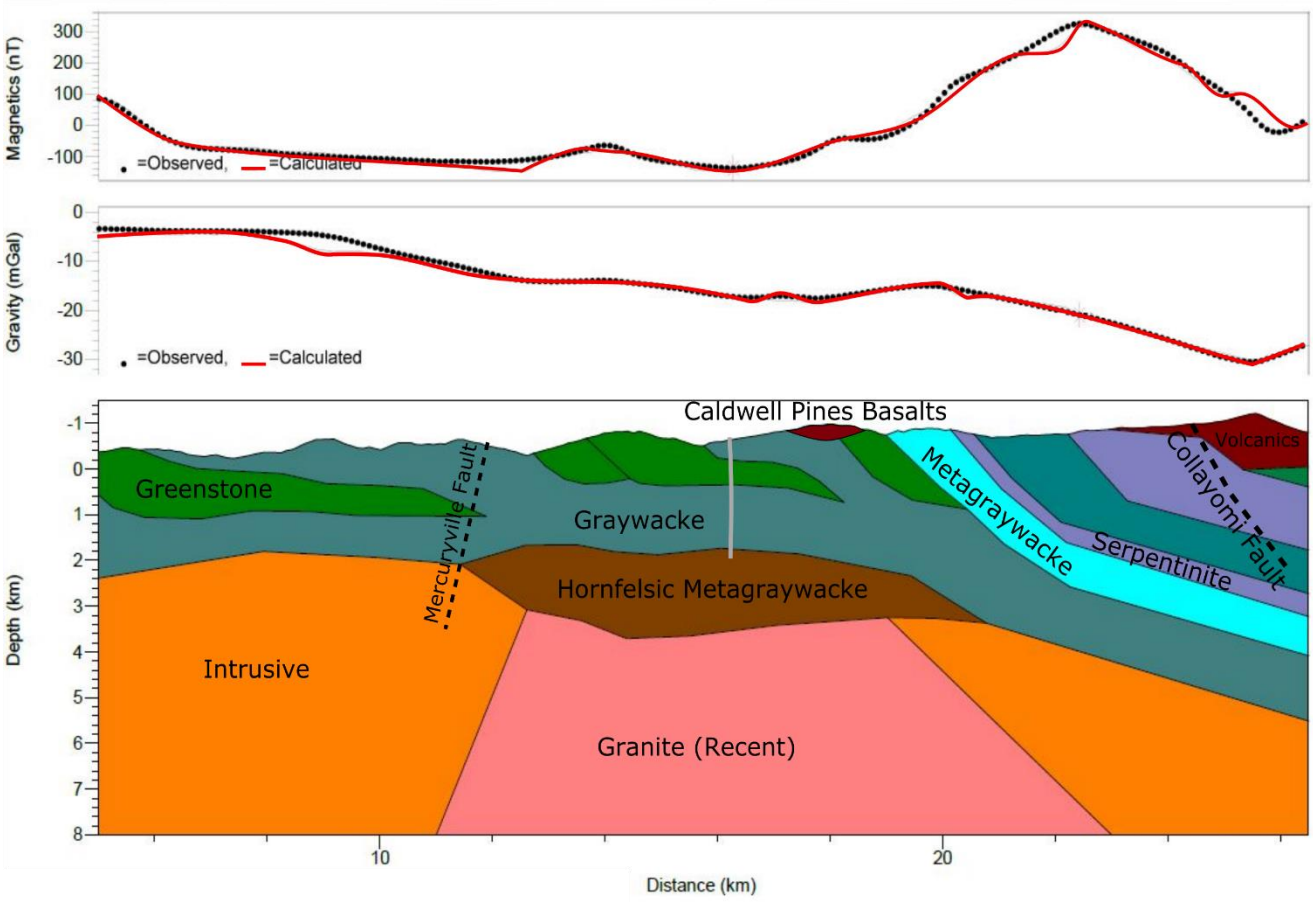

Figure 2: Interpreted potential field model along profile A in Figure 1, gray line is the approximate location of the EGS wells. Note this is a very preliminary and basic model. The important aspect of the model is that a low-density, low-susceptibility body is needed below 5 km depth to fit the potential field data. Geometry of this body is not well constrained in this model.

3. RESULTS

Comparing R1 to existing 3D geologic models of The Geysers (Hartline et al., 2016; Forson et al., 2016), R1 is a superposition of 2 structures as supported by the potential field model (Figure 2). The top of R1 is between 45-60 Ohm-m and coincides with the top of the steam reservoir estimated from drill holes. Resistivities greater than 60 Ohm-m coincides with the known location of the felsite.

Graywacke is typically a resistive rock (Bertrand et al, 2013), and elsewhere in the Franciscan Assemblage is on the order of 100 Ohm-m (Bedrosian et al., 2002). Petrology indicates that saline fluids, past and present (Lambert et al., 1992; Truesdell et al., 1993; Hulen et al., 1997), whether connate or magmatic, are left as fluid inclusions in the graywacke (Lutz et al, 2012). Matrix porosity of the reservoir is estimated to be on the order of 1% and fracture dominated porosity is 1-3% (Thompson & Gunderson, 1992; Walters et al., 1992; Lutz et al., 2012). These observations suggest that the lower resistivity of the graywacke is related to the presence or remnants of saline fluids in the minimal pore space and fractures. Though being a steam-dominated system, the resistivity of the graywacke is not as low as in a fluid dominated system, like that in the Taupo geothermal field in New Zealand (Bertrand et al., 2013).

Felsite resistivity changes from less resistive on the outer parts (70 Ohm-m) to more resistive on the inner parts (>100 Ohm-m), similar to a resistivity model by Stanley et al., (1998). The outer part is also lower than expected for granitic plutonic rocks. For a dry granite at around 300 °C (Dalrymple et al., 1999) the expected resistivity would be on the order of 10^6 Ohm-m (Olhoeft, 1981). However, for a

matrix saturated granite under similar conditions and a fluid salinity of 0.1 molar NaCl, the expected resistivity would be on the order of 10 Ohm-m (Olhoeft, 1981). Thus, the felsite is either not fully saturated or the molarity of the fluids is less than 0.1 molar to be slightly more resistive than 10 Ohm-m. Moreover, near the center of the felsite the pores are likely to be smaller and less saturated than the outer part of the felsite assuming temperature remains the same.

The structure of the felsite is bounded on the west side by the Mercuryville fault system. Some geologic cross-sections have the Mercuryville Fault dip to the east (e.g. Garcia et al., 2016) and others have the fault dip to the west (e.g. Stanley et al., 1998). The 3D resistivity model suggests that the Mercuryville Fault is a steep, west dipping fault that extends to at least 5 km depth, which is consistent with seismicity and the 3D model of Hartline et al. (2016). The Mercuryville Fault, or parallel fault (Hulen & Norton, 1996), could have allowed magma to intrude as a dike. As the magma reached zones of lower pressure expanded into a similar shape observed in the resistivity model. The felsite appears to extend to the north just beyond the Aidlin Power Plant, with a dip to the north such that the depth to the top of the felsite is 3 km. This northern extension is narrow and slightly less resistive than the rest of the felsite.

R2, the northeastern extension of the felsite under the HDR, is also less resistive than the rest of the felsite. R2 appears to be constrained between 2-4 km depth, is narrow (2-3 km wide), and between 45-80 Ohm-m. Again, the upper part of this extension is likely part of the steam-dominate reservoir, but high-temperature alteration below 2.5 km suggests that the lower part has higher temperatures than the rest of the felsite. Assuming conditions are similar, the expected temperature would be on the order of 400 °C (Olhoeft, 1981) at 3 km depth. This agrees with existing estimates of the HDR (Garcia et al., 2012; Garcia et al., 2016; Rutqvist et al., 2016). Being hotter than the rest of the felsite would suggest that R2 is younger and the potential conductive heat source for the HDR.

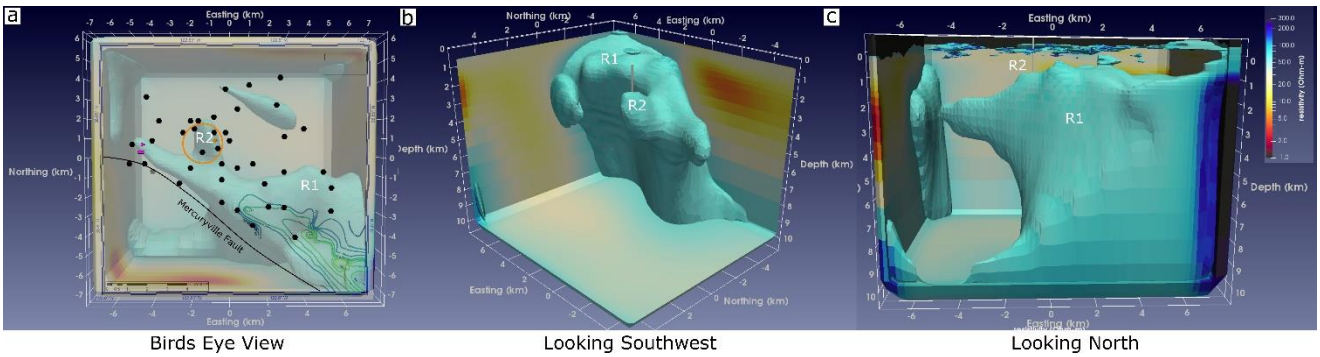

Figure 3: Images of R1 and R2 from the electrical resistivity model showing the iso-surface for resistivities larger than 65 Ohm-m . a) shows a bird's eye view with known felsite contours in green (shallow) to blue (deeper), black dots are MT stations, other symbols are the same as Figure 1. b) shows the resistive iso-surface looking towards the southwest. The gray cylinder is the approximate location of the EGS project. c) shows the resistive iso-surface looking to the north.

C1, is a conductive anomaly under R2 and the Caldwell Pines basalts (1.66 Ma; Donelly-Nolan et al., 1981). The shape of C1 is suggestive of a deeper part that extends into the near the surface. The deeper part of C1, below 5 km, is between 25-30 ohm-m, and appears to be connected to a larger, possibly magmatic (e.g. Walters et al., 1992), conductor to the east. Truesdell et al., (1993) suggest that a possible magmatic source lies under Caldwell Pines, which could be C1. If C1 is a zone of partial melt, the percent melt can be estimated from the resistivity (Pommier & Le-Trong, 2011). Assuming the melt has evolved to a granitic composition like the felsite with temperature on the order of 700 °C and a water content of 1%, the melt resistivity is expected to be approximately 5 Ohm-m. Using a modified Archie's law with a connectivity exponent of 1.05 (Gaillard & Marziano, 2005) gives a melt percent of approximately 10% for the lower part of C1. This is likely an upper bound because drier and cooler melts will be more resistive.

The connection between the lower part of C1 and the upper part above 5 km has been tested statistically. RMS of the data fits increase when the connection is removed and set to background levels in the resistivity model. Interestingly, the connecting zone is aseismic, consistent with high temperature, softened rock, and is characterized by a low V_p/V_s ratio of 1.52-1.58 (Gritto et al., 2013) relative to that in the surrounding resistant rock (R1). It is possible that deep-to-shallow connection is a 'paleo' pathway marking the ascent of the Caldwell Pines basalt from the magmatic source to the surface, resulting in quartz-rich veins lowering the V_p/V_s ratio.

4. SUMMARY

A 3D resistivity model developed from MT measurements has imaged the potential heat source for the HDR in the northwest Geysers. An extension of the felsite is imaged 3 km below the HDR that is slightly less resistive than the rest of the upper portion of the felsite, indicating warmer temperatures at depth. This is likely the thermally conductive rock responsible for heating the HDR. An electrically conductive zone below 5 km depth could be a zone of <10% partial melt responsible for providing heat to the felsite. An electrically conductive connection from this deeper anomaly is likely the remnant pathway of the Caldwell Pines basalts.

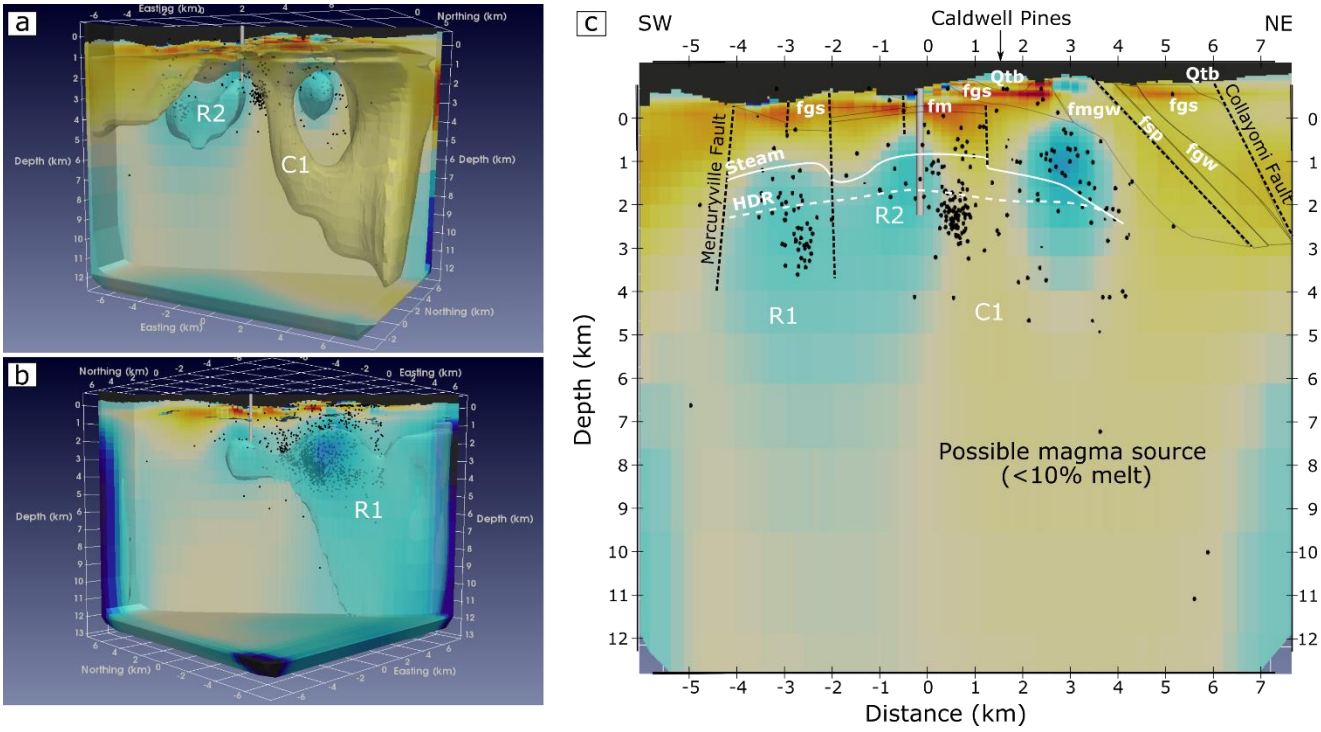

Figure 3: Cross sections of the electrical resistivity model across the EGS and HDR, same color scale as Figure 2. Black dots are earthquake hypocenters (Waldhauser & Schaff, 2008). a) Cross section along line A in Figure 1 with iso-surfaces at <30 Ohm-m and >65 Ohm-m. b) Cross section along line B in Figure 1 with same iso-surfaces. c) Cross section along line A in Figure 1, with faults (dotted lines), lithologic units, and top of stem and the HDR from Garcia et al., 2012. Qtb – Quaternary Basalt, Fgs – greenstone, Fm – chert, Fgw – graywacke, Fmgw – metagraywacke, Fsp – serpentinite.

ACKNOWLEDGMENTS

The authors would like to thank Benjamin Grober, Zach Palmer, and Claire Peacock for helping with MT field work, and Richard Black and Kevin Talkington from Calpine for helping with permitting. MT and gravity data are available upon request and are planned to be made publicly available on Science Base (https://www.sciencebase.gov/catalog/) in March 2019. Any use of trade, firm, or product names is for descriptive purposes only and does not imply endorsement by the U.S. Government.

REFERENCES

Bedrosian, P. A., Unsworth, M. J., Egbert, G., Magnetotelluric imaging of the creeping segment of the San Andreas Fault near Hollister, *Geophysical Research Letters*, **29**, (2002), 1-4.

Bertrand, E. A., Caldwell, T. G., Hill, G. J., Bennie, S. L., Soengkono, S., Mangetotelluric imaging of the Ohaaki geothermal system, New Zealand: implications for locating basement permeability, *Journal of Volcanology and Geothermal Research*, **268**, (2013), 36-45.

Blakely. R.J. and Stanley, W.D., The Geysers magma chamber, California: constraints from gravity data, density measurements, and well information, *Geothermal Resources Council Transactions*, **17**, (1993), 227-233.

Blakely, R. J., Potential theory in gravity and magnetic applications, Cambridge University Press, New York, (1995).

Boyle, K., Zoback, M., Stress and fracture orientation in the northwest Geysers geothermal field, 38th Workshop on Geothermal Reservoir Engineering, Stanford University, Stanford, CA, (2013).

Chave, A. D. and Thomson, D. J., Bounded influence estimation of Magnetotelluric response functions, *Geophysical Journal International*, **157**, (2004), 988-1006.

Dalrymple, G. B., Grove, M., Lovera, O. M., Harrison, T. M., Hulen, J. B., Lanphere, M. A., Age and thermal history of The Geysers plutonic complex (felsite unit) Geysers geothermal field, California: a $^{40}Ar/^{39}Ar$ and U–Pb study, *Earth and Planetary Science Letters*, **173**, (1999), 285-298.

Denlinger, R. P. and Kovach, R. L., Three-dimensional gravity modeling of The Geysers hydrothermal system and vicinity, northern California, *Geological Society of America Bulletin*, **92**, (1981), 404-411.

Donnelly-Nolan, Julie M., B. Carter Hearn Jr, Garniss H. Curtis, and Robert E. Drake. Geochronology and evolution of the Clear Lake Volcanics. U.S. Geological Survey Professional Paper 1141, (1981), 47-60.

Forson, C., Sadowski, A., Walters, M., Hartline, C., Geologic Map of The Geysers Geothermal Field California, 41st Workshop on Geothermal Reservoir Engineering, Stanford University, Stanford, CA, (2016), 1732-1743.

Gaillard, F. and Marziano, G. I., Electrical conductivity of magma in the course of crystallization controlled by their residual liquid composition, *Journal of Geophysical Research*, **110**, (2005), B06204.

Garcia, J., Walters, M., Beall, J., Hartline, C., Pingol, A., Pistone, S., Wright, M., Overview of the Northwest Geysers EGS demonstration project, 37th Workshop on Geothermal Reservoir Engineering, Stanford University, Stanford, CA, (2012).

Garcia, J., Hartline, C., Walters, M., Wright, M., Rutqvist, J., Dobson, P. F., Jeanne, P., The Northwest Geysers EGS Demonstration Project, California – Part 1: characterization and reservoir response to injection, *Geothermics*, **63**, (2016), 97-119.

Godson, R. H. and Plouff, D., BOUGER version 1.0, a microcomputer gravity-terrain-correction program, U.S. Geological Survey Open-File Report 88-644-B, (1988).

Gritto, R., Yoo, S. H., Jarpe, S. P., Three-dimensional seismic tomography at The Geysers geothermal field, CA, USA, 38th Workshop on Geothermal Reservoir Engineering, Stanford University, Stanford, CA, (2013).

Hartline, C. S., Walters, M. A., Wright M. C., Forson, C. K, Sadowski, A. J., Three-dimensional structural model building, induced seismicity analysis, drill analysis and reservoir management at The Geysers Geothermal Field, Northern California, 41st Workshop on Geothermal Reservoir Engineering, Stanford University, Stanford, CA, (2016), 1-12.

Hulen, J. B. and Nielson, D. L., The Geysers felsite, *Geothermal Resources Council Transactions*, **20**, (1996) 295–306.

Hulen, J. B., Heizler, M. T., Stimac, J. A., Moore, J. N., Quick, J. C., New constraints on the timing of magmatism, volcanism, and the onset of vapor-dominated conditions at The Geysers steam field, California, 22nd Workshop on Geothermal Reservoir Engineering, Stanford University, Stanford, CA, (1997).

Jeanne, P., Rutqvist, J., Vasco, D. W., Garcia, J., Dobson, P. F., Walters, M., Hartline, C., Borgia, A., A 3D hydrogeological and geomechanical model of the Enhanced Geothermal System at The Geysers, California, *Geothermics*, **51**, (2014), 240-252.

Jeanne, P., Rutqvist, J., Hutchings, L., Singh, A., Dobson, P. F., Walters, M., Hartline., C., Garcia, J., Degradation of the mechanical properties imaged by seismic tomography during an EGS creation at The Geysers (California) and geomechanical modeling, *Physics of the Earth and Planetary Interiors*, **240**, (2015), 82-94.

Julian, B.R., Ross, A., Foulger, G. R., Evans, J. R., Three-dimensional seismic image of a geothermal reservoir: The Geysers, California, *Geophysical Research Letters*, **23**, (1996), 685-688.

Kelbert, A., Meqbel, N., Egbert, G. D., Tandon, K., ModEM: A modular system for inversion of electromagnetic geophysical data, *Computers & Geoscience*, **66**, (2014), 40-53.

Kreiger, L. and Peacock, J. R., MTpy: a python toolbox for magnetotellurics, *Computers & Geoscience*, **72**, (2014), 167-175.

Lambert, S. J. and Epstein, S., Stable-isotope studies of rocks and secondary minerals in a vapor-dominated hydrothermal system at The Geysers, Sonoma County, California, *Journal of Volcanology and Geothermal Research*, **53**, (1992), 199-226.

Lin, G., Wu, B., Seismic velocity structure and characteristics of induced seismicity at The Geysers geothermal field, eastern California, *Geothermics*, **71**, (2018), 225-233.

Lutz, S. J., Walters, M., Pistone, S., Moore, J. N., New insights into the high-temperature reservoir, Northwest Geysers, *Geothermal Resources Council Transactions*, **36**, (2012), 907-916.

McLaughlin, R.J., Preliminary geologic map and structural sections of the central Mayacmas Mountains and The Geysers steam field, Sonoma, Lake, and Mendocino Counties, California: US. Geological Survey Open-File Map 78-389, (1978), scale 1:24,000.

McLaughlin, R.J., Tectonic setting of pre-Tertiary rocks and its relation to geothermal resources in the Geysers-Clear Lake area, California: US. Geological Survey Professional Paper 1141, (1981), p. 3-23.

Olhoeft, G. R., Electrical properties of granite with implications for the lower crust, *Journal of Geophysical Research*, **86**, (1981), 931-936.

Pommier, A. and Le-Trong, E., "SIGMELTS": a web portal for electrical conductivity calculations in geosciences, *Computers & Geoscience*, **37**, (2011), 1450-1459.

Rutqvist, J., Dobson, P. F., Garcia, J., Hartline, C., Jeanne, P., Oldenburg, C. M., Vasco, D. W., Walters, M., The Northwest Geysers EGS Demonstration Project, California: pre-stimulation modeling and interpretation of the stimulation, *Mathematical Geosciences*, **47**, (2015), 3-29.

Rutqvist, J., Jeanne, P., Dobson, P. F., Garcia, J., Hartline, C., Hutchings, L., Singh, A., Vasco, D. W., Walters, M., The Northwest Geysers EGS Demonstration Project, California – Part 2: modeling and interpretation, *Geothermics*, **63**, (2016), 120-138.

Schriener, A., Suemnicht, G. A., Subsurface intrusive rocks at The Geysers geothermal area, California, U. S. Geological Survey Open-File Report 81-355, (1981), 295-302.

Simpson, R. W., Jachens, R. J., Blakely, R. J., Saltus, R. W., A new isostatic residual gravity map of the conterminous United States with a discussion on the significance of isostatic residual gravity anomalies, *Journal of Geophysical Research*, **91**, (1985), 8348-8372.

Stark, M., Seismic evidence for a long-lived Enhance Geothermal System (EGS) in the Northern Geysers Reservoir, *Geothermal Resources Council Transactions*, **27**, (2003), 727-731.

Stanley, W. D., Dallas, B. J., Hearn, B. C., Preliminary results of geoelectrical investigations near Clear Lake, California, U. S. Geological Survey Open-File Report, (1973), 1-22.

Stanley, W. D. and Blakely, R. J., The Geysers-Clear Lake geothermal area, California – an updated geophysical perspective of heat sources, *Geothermics*, **24**, (1995), 187-221.

Stanley, W. D., Benz, H. M., Walters, M. A., Villasenor, A., Rodriguez, B. D., Tectonic controls on magmatism in The Geysers-Clear Lake region: evidence from new geophysical models, *GSA Bulletin*, **110**, (1998), 1193-1207.

Stimac, J. A., Goff, F., Wohletz, K., Thermal modeling of the Clear Lake magmatic-hydrothermal system, California, USA, *Geothermics*, **30**, (2001), 349-390.

Tezel, T., Julian, B. R., Foulger, G. R., Nunn, C., Mhana, N., Preliminary 4D seismic tomography images for The Geysers, 2008-2014, 41st Workshop on Geothermal Reservoir Engineering, Stanford University, Stanford, CA, (2016).

Thompson, R.C., and Gunderson, R.P., The orientation of steam-bearing fractures at The Geysers geothermal field *in* Monograph on The Geysers geothermal field (C. Stone, ed.), *Geothermal Resources Council Special Report 17*, (1992), 65-68.

Truesdell, A., Walters, M. A., Kennedy, M., Lippmann, M., An integrated model for the origin of The Geysers geothermal field, *Geothermal Resources Council Transactions*, **17**, (1993), 1-8.

U.S. Geological Survey, Aeromagnetic map of the Clear Lake region on parts of the Santa Rosa and Ukiah 1 degree by 2 degree quadrangles, California, U.S. Geological Survey Open-File Report 96-691, (1996).

Waldhauser, F. and D.P. Schaff, Large-scale relocation of two decades of Northern California seismicity using cross-correlation and double-difference methods, *Journal of Geophysical Research*, **113**, (2008), B08311.

Walters, M.A., Sternfeld, J.N., Haizlip, J.R., Drenick, A.F., and Combs, J., A vapor-dominated, high-temperature reservoir at The Geysers, California *in* Monograph on The Geysers geothermal field (C. Stone, ed.): *Geothermal Resources Council Special Report 17*, (1992), 43-53.

Williams, C. F., Galanis, S. P., Moses, T. H., Grubb, F. V., Heat-flow studies in the northwest Geysers geothermal field, California, *Geothermal Resources Council Transactions*, **17**, (1993), 281-287.

Vasco, D.W., Rutqvist, J., Ferretti, A., Rucci, A., Bellotti, F., Dobson, P., Oldenburg, C., Garcia, J., Walters, M., Hartline, C., Monitoring deformation at The Geysers geothermal field, California using C-band and X-band interferometric synthetic aperture radar. *Geophysical Research Letters*, 40, (2013), 2567-2572.